

Scalable Inference of System-level Models from Component Logs

Donghwan Shin*, Salma Messaoudi*, Domenico Bianculli*, Annibale Panichella*, Lionel Briand*,
and Raimondas Sasnauskas†

*University of Luxembourg, Luxembourg

†SES, Luxembourg

Abstract—Behavioral software models play a key role in many software engineering tasks; unfortunately, these models either are not available during software development or, if available, they quickly become outdated as the implementations evolve. Model inference techniques have been proposed as a viable solution to extract finite state models from execution logs. However, existing techniques do not scale well when processing very large logs, such as system-level logs obtained by combining component-level logs. Furthermore, in the case of component-based systems, existing techniques assume to know the definitions of communication channels between components. However, this detailed information is usually not available in the case of systems integrating 3rd-party components with limited documentation.

In this paper, we address the scalability problem of inferring the model of a component-based system from the individual component-level logs, when the only available information about the system are high-level architecture dependencies among components and a (possibly incomplete) list of log message templates denoting communication events between components. Our model inference technique, called SCALER, follows a divide and conquer approach. The idea is to first infer a model of each system component from the corresponding logs; then, the individual component models are merged together taking into account the dependencies among components, as reflected in the logs. We evaluated SCALER in terms of scalability and accuracy, using a dataset of logs from an industrial system; the results show that SCALER can process much larger logs than a state-of-the-art tool, while yielding more accurate models.

Index Terms—Model inference, Finite state machines, Logs, Components

I. INTRODUCTION

Behavior models of software system components play a key role in many software engineering tasks, such as program comprehension [1], test case generation [2], and model checking [3]. Unfortunately, such models either are scarce during software development or, if available, they quickly become outdated as the implementations evolve, because of the time and cost involved in generating and maintaining them [4].

One possible way to overcome the lack of software models is to use *model inference* techniques, which extract models—typically in the form of (some type of) Finite State Machine (FSM)—from execution logs. Although the problem of inferring a minimal FSM is NP-complete [5], there have been several proposals of polynomial-time approximation algorithms to infer FSMs [5]–[7] or richer variants, such as gFSM (guarded FSM) [8], [9] and gFSM extended with transition probabilities [10], to obtain more faithful models.

Although the aforementioned model inference techniques are fast and accurate enough for relatively small programs, all of them suffer from scalability issues, due to the intrinsic computational complexity of the problem. This leads to out-of-memory errors or extremely long, unpractical execution time when processing very large logs [11], such as system-level logs obtained by combining (e.g., through linearization) component-level logs. A recent proposal [7] addresses the scalability issue using a distributed FSM inference approach based on MapReduce. However, this approach requires to encode the data to be exchanged between mappers and reducers in the form of key-value pairs. Such encoding is application-specific; hence, it cannot be used in contexts—like the one in which this work has been performed—in which the system is treated as a black-box (i.e., the source code is not available), with limited information about the data recorded in the individual components logs.

Another limitation of state-of-the-art techniques is that they cannot infer, from component-level logs, a system-level model that captures both the individual behaviors of the system’s components and the interactions among them. Such a scenario can be handled with existing model inference techniques for distributed systems, such as CSight [12], which typically assume the availability of channels definitions, i.e., the exact definition of which events communicate with each other between components. However, this information is not available in many practical contexts, where the system is composed of heterogenous, 3rd-party components, with limited documentation about the messages exchanged between components and the events recorded in logs.

In this paper, we address the scalability problem of inferring the model of a component-based system from the individual component-level logs (possibly coming from multiple executions), when the only available information about the system are high-level architecture dependencies among components and a (possibly incomplete) list of log message templates denoting communication events between components. Our goal is to infer a system-level model that captures not only the components’ behaviors reflected in the logs but also the interactions among them.

Our approach, called SCALER, follows a *divide and conquer* strategy: we first infer a model of each component from the corresponding logs using a state-of-the-art model inference technique, and then we “stitch” (i.e., we do a peculiar type

of merge) the individual component models into a system-level model by taking into account the dependencies among the components, *as reflected in the logs*. The rationale behind this idea is that, though existing model inference techniques cannot deal with the size of all combined component logs, they can still be used to infer the models of individual components, since their logs are sufficiently small. In other words, *SCALER* tames the scalability issues of existing techniques by applying them on the smaller scope defined by component-level logs.

We implemented *SCALER* in a prototype tool, which uses MINT [8], a state-of-the-art technique for inferring gFSM, to infer the individual component-level models. We evaluate the scalability (in terms of execution time) and the accuracy (in terms of recall and specificity) of *SCALER* in comparison with MINT (fed with system-level logs reconstructed from component-level logs), on seven proprietary datasets from one of our industrial partners in the satellite domain. The results show that our approach *SCALER* is about 245 times (on average) faster and can process larger logs than MINT. It generates nearly correct (with specificity always higher than 0.96) and largely complete models (with an average recall of 0.79), achieving higher recall than MINT (with a difference ranging between +25 *pp* and +56 *pp*, with *pp*=percentage points) while retaining similar specificity.

To summarize, the main contributions of this paper are:

- the *SCALER* approach for taming the scalability problem of inferring the model of a component-based system from the individual component-level logs, especially when only limited information about the system is available;
- a publicly available implementation of *SCALER*¹;
- the empirical evaluation, in terms of scalability and accuracy, of *SCALER* and its comparison with a state-of-the-art approach.

The rest of the paper is organized as follows. Section II gives the basic definitions of logs and models that will be used throughout the paper. Section III illustrates the motivating example. Section IV describes the different steps of the core algorithm of *SCALER*. Section V reports on the evaluation of *SCALER*. Section VI discusses related work. Section VII concludes the paper and provides directions for future work.

II. BACKGROUND

This section provides the basic definitions for the main concepts that will be used throughout the paper.

Logs: A log is a sequence of log entries; a log entry contains a timestamp (recording the time at which the logged event occurred) and a log message (with run-time information related to the logged event). A log message is a block of free-form text that can be further decomposed [13] into a fixed part called event template, characterizing the event type, and a variable part, which contains tokens filled at run time with the values of the event parameters. For example, given the log entry `20181119:14:26:00 send OK to comp1`, the timestamp is 20181119:14:26:00, the event template



Fig. 1. The components of the example system and their dependencies

contains the fixed words **send** and **to**, while the tokens `OK` and `comp1` are the values of the event parameters. More formally, let ET be the set of all events that can occur in a system and V be the set of all mappings from events parameters to their concrete values, for all events $et \in ET$; a log L is a sequence of log entries $\langle e_1, \dots, e_n \rangle$, with $e_i = (ts_i, et_i, v_i)$, $ts_i \in \mathbb{N}$, $et_i \in ET$, and $v_i \in V$, for $i = 1, \dots, n$. We denote the log of a component c_X with L_{c_X} . To denote individual log entries, we use the notation $e_{i,j}^k$ for the i -th log entry of component k in the j -th execution; we drop the subscript j when it is clear from the context.

Guarded Finite State Machines: We represent the models inferred for a system as guarded Finite State Machines (gFSMs). A gFSM is a tuple $m = (S, ET, G, \delta, s_0, F)$, where S is a finite set of states, ET is the set of system events defined above, G is a finite set of guard functions of the form $g: V \rightarrow \{0, 1\}$, δ is the transition relation $\delta \subseteq S \times ET \times G \times S$, $s_0 \in S$ is the initial state, $F \subseteq S$ is the set of final states. Informally, a gFSM is a finite state machine whose transitions are triggered by the occurrence of an event and are guarded by a function that evaluates the values of the event parameters. More specifically, a gFSM m makes a guarded transition from a state $s \in S$ to a state $s' \in S$ when reading an input log entry $e = (ts, et, v)$, written as $s \xrightarrow{e} s'$, if $(s, et, g, s') \in \delta$ and $g(v) = 1$. We say that m *accepts* a log $l = \langle e_1, \dots, e_n \rangle$ if there exists a sequence of states $\langle \gamma_0, \dots, \gamma_n \rangle$ such that (1) $\gamma_i \in S$ for $i = 0, \dots, n$, (2) $\gamma_0 = s_0$, (3) $\gamma_{i-1} \xrightarrow{e_i} \gamma_i$ for $i = 1, \dots, n$, and (4) $\gamma_n \in F$.

III. MOTIVATIONS

In this section, we discuss the motivations for this work using an example based on a real system from one of our industrial partners in the satellite domain. We consider a simplified version of a satellite ground control system, composed of the four components shown in Figure 1: *TC*, the module handling tele-commands for the satellite, which is also the entry point of the system; *MUX*, a multiplexer combining different tele-commands into a single communication stream; *CHK*, the module validating the tele-commands parameters before they are sent to the satellite; *GW*, the gateway managing the connections between the satellite and the ground control system. Figure 1 also shows the architectural dependencies among components; for example, the arrow from component *TC* to component *MUX* indicates that *TC* *uses* (or *invokes*) an operation provided by *MUX*. Every execution of the system generates a set of logs, with one log for each component; Figure 2 depicts the logs of the four system components generated in two executions; for space reasons, the format of timestamps has been compressed.

To infer a model from these individual component logs, one could use existing model inference techniques for distributed systems, such as CSight [12]. These techniques typically

¹The open-source license is currently being reviewed by our legal team.

CMP	Execution 1	Execution 2
TC	$e_{1,1}^{TC} = 14:26:01$ sending X via f0	$e_{1,2}^{TC} = 14:30:11$ sending Y via f1
	$e_{2,1}^{TC} = 14:26:02$ TC accepted	$e_{2,2}^{TC} = 14:30:12$ wait message
MUX	$e_{1,1}^{MUX} = 14:26:01$ initialize	$e_{1,2}^{MUX} = 14:30:11$ initialize
	$e_{2,1}^{MUX} = 14:26:01$ commandName = X	$e_{2,2}^{MUX} = 14:30:12$ commandName = Y
	$e_{3,1}^{MUX} = 14:26:01$ commandName = X	$e_{3,2}^{MUX} = 14:30:12$ data flow ID = f1
	$e_{4,1}^{MUX} = 14:26:01$ data flow ID = f0	$e_{4,2}^{MUX} = 14:30:12$ send = no
GW	$e_{5,1}^{MUX} = 14:26:02$ send= ok	
	$e_{1,1}^{GW} = 14:26:01$ encrypt TC_01	$e_{1,2}^{GW} = 14:30:12$ reject command
CHK	$e_{1,1}^{CHK} = 14:26:01$ mode 1	$e_{1,2}^{CHK} = 14:30:11$ mode 0
	$e_{2,1}^{CHK} = 14:26:02$ automatic config	

Log Message Templates

*tmp ₁ = sending v ₁ via v ₂	*tmp ₂ = TC accepted	*tmp ₃ = wait message
*tmp ₄ = initialize	tmp ₅ = cmdName = v ₁	tmp ₆ = data flow ID = v ₁
*tmp ₇ = send = v ₁	*tmp ₈ = encrypt v ₁	*tmp ₉ = reject command
*tmp ₁₀ = mode v ₁	*tmp ₁₁ = automatic config	

Fig. 2. (top) Component logs generated by two executions of the example system; (bottom) Log message templates extracted from components logs (communication message templates are marked with an asterisk).

assume the availability of channels definitions, i.e., the exact definition of which events communicate to each other between components. However, this information is not available in many practical contexts, including ours, where the system is composed of heterogenous, 3rd-party components, with limited documentation. More specifically, the only available information about the system are high-level architecture dependencies among components (like those in Figure 1) and a (possibly incomplete) list of communication events, without knowing exactly how events communicate with each other. Due to this limited information, we cannot use existing techniques for model inference for distributed systems.

Another approach towards model inference would be to reconstruct a system-level log from the individual component logs and use non-distributed model inference techniques such as MINT [8] or GK-tail+ [9]. However, such approaches typically suffer from scalability issues due to the underlying algorithms they use. For example, the main algorithm used in MINT has worst-case time complexity that is cubic in the size of the inferred model [14]; the algorithm used for removing non-determinism from models can exhibit, based on our preliminary evaluation, deep recursion that causes stack overflows and makes MINT crash. Furthermore, GK-tail+ is not publicly available and the largest log on which it was evaluated contained 11386 log entries. Since the system of our industrial partner can generate, when considering all the components, logs with more than 30000 entries, there is need for a scalable model inference technique that can process component logs.

IV. SCALABLE MODEL INFERENCE

Our technique for system model inference from component logs follows a *divide and conquer* approach. The idea is to first infer a model of each system component from the corresponding logs; then, the individual component models are merged together taking into account the dependencies among components, *as reflected in the logs*. We call this process *SCALER*. The rationale behind our technique is that though existing (log-based) model inference techniques cannot deal with

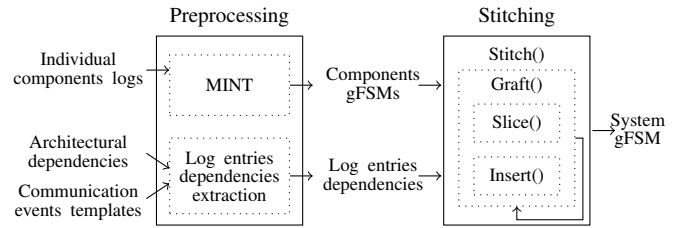


Fig. 3. Workflow of the *SCALER* technique

the size of all combined component logs, they can still be used to accurately infer the models of individual components, since their logs are sufficiently small for the existing model inference techniques to work. The challenge is then how to “stitch” together the models of the individual components to build a system model that reflects not only the components behavior but also their dependencies, while preserving the accuracy of the component models. For example, simply appending one component model after the other perfectly preserves the accuracy of the inferred component models, but it significantly loses the dependencies between components. On the other hand, performing a parallel composition of automata on the component models (based on the dependencies between components) loses the accuracy of the component models because of the over-generalization caused by the parallel composition. To solve this problem, we develop a set of novel algorithms that take into account the dependencies between components while preserving the component models as much as possible.

Figure 3 outlines the workflow of *SCALER*. The technique takes as input the logs of the different components, possibly coming from multiple executions, a description of the architectural dependencies among components, and a list of log message templates denoting communication events between components; it returns a system level gFSM. *SCALER* is composed of two stages, *pre-processing* and *stitching*, described in the following subsections.

A. Pre-processing Stage

This stage prepares two intermediate outputs, *component-level models* and *log entries dependencies*, which will be used by the main stitching stage.

Inferring Component Models: For each component, we infer a component-level model based on the corresponding logs using MINT [8], an open-source state-of-the-art tool.

MINT takes as input (1) the logs produced by the individual component for which one wants to infer the model and (2) the templates of the events recorded in the component logs. The event templates are required to parse the log entries, to retrieve the actual events and their parameters. Nevertheless, often such templates are not available or documented. This situation is typical when dealing with 3rd-party, black-box components—as it is the case for the ground control system used by our industrial partner—and it is known in the literature as the log message format identification problem. We use MoLFI [13],

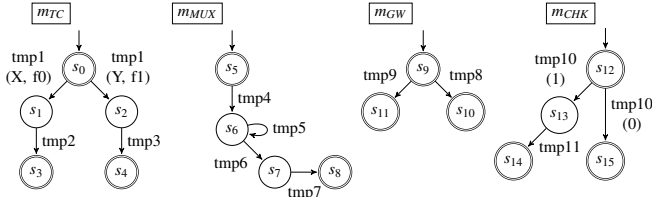


Fig. 4. Component-level gFSMs inferred by MINT from the logs shown in Table 2

a state-of-the-art solution for this problem, to derive the event templates that are then used by MINT; as an example, the box at the bottom of Figure 2 shows the templates produced by MoLFI from the logs of our running example.

The models inferred by MINT are gFSMs; Figure 4 shows the component-level gFSMs inferred by MINT for the four components of our running example. We use a compact notation for the guards on the event parameters labeling the guarded transitions; for example, in the gFSM of *TC* (i.e., m_{TC}), the guard $(X, \neq 0)$ stands for $(v_1 = "X", v_2 = "\neq 0")$.

Identifying Log Entries Dependencies: A system-level model of a component-based system has to capture not only the behavior of the individual components but also the intrinsic behavioral dependencies among them. For example, considering the fact that *TC* invokes *MUX* as shown in Figure 1, one could speculate that the event recorded in entry $e_{1,1}^{TC}$ could lead to the event recorded in entry $e_{1,1}^{MUX}$ in Figure 2; if this is the case, the model should reflect this dependency, which we call *log entries dependency*.

Log entries dependencies can be extracted from the source code by means of program analysis or from existing models such as UML Sequence Diagrams [15], [16]. However, the extraction is infeasible when the source code is not available and the documentation is limited. This is the case for the example system provided by our industrial partner: the source code of 3rd-party components is not available, the architectural documentation only includes coarse-grained dependencies (like those shown in Figure 1), and the only additional information is the knowledge of domain experts, who can provide a (possibly incomplete) list of log message templates corresponding to events related to the “communication” between components (like those marked with an asterisk in Figure 2). To solve this issue, we present a simple heuristic that identifies log entries dependencies from the coarse-grained component dependencies, the list of communication event templates, and the individual component logs.

The idea at the basis of our heuristic is that, if there is an architectural dependency from a component c_X to another component c_Y (representing the use of c_Y by c_X), then all log entries of c_Y are ultimately the consequences of the log entries of c_X . The identification of log entries dependencies boils down to finding out, for each pair of components c_X and c_Y with c_X using c_Y , which log entries of c_Y are the consequences of which log entry of c_X . We observe that, among the log entries of c_Y , the communication (events recorded in) log entries are invoked directly from c_X . Furthermore, given the

TABLE I
EXTRACTED LOG ENTRIES DEPENDENCIES FOR THE RUNNING EXAMPLE

Execution	Log entry dependencies
Exec1	$e_1^{TC} \rightsquigarrow \langle e_1^{MUX}, e_2^{MUX}, e_3^{MUX}, e_4^{MUX} \rangle$
	$e_1^{TC} \rightsquigarrow \langle e_1^{CHK} \rangle, e_2^{TC} \rightsquigarrow \langle e_5^{MUX} \rangle$
	$e_2^{TC} \rightsquigarrow \langle e_2^{CHK} \rangle, e_4^{MUX} \rightsquigarrow \langle e_1^{GW} \rangle$
Exec2	$e_1^{TC} \rightsquigarrow \langle e_1^{MUX}, e_2^{MUX}, e_3^{MUX} \rangle$
	$e_1^{TC} \rightsquigarrow \langle e_1^{CHK} \rangle, e_2^{TC} \rightsquigarrow \langle e_4^{MUX} \rangle$
	$e_4^{MUX} \rightsquigarrow \langle e_1^{GW} \rangle$

timestamp² of a communication log entry ce^Y of c_Y , we observe that ce^Y communicated with the most recent communication log entry ce^X of c_X . Based on these observations, we say that ce^X (*communicatively*) *leads-to* ce^Y , denoted with $ce^X \rightsquigarrow_c ce^Y$, only if (1) the timestamp of ce^X is less than or equal to the one of ce^Y and (2) the timestamp difference between ce^X and ce^Y is the minimum among all pairs of the communication log entries of c_X and c_Y . In our running example, given the list of templates corresponding to (log entries of) communication events: tmp_1 , tmp_2 , tmp_4 , and tmp_7 , if we consider the architectural dependency from *TC* to *MUX* and focus on the first execution, we say that $e_1^{TC} \rightsquigarrow_c e_1^{MUX}$ and $e_2^{TC} \rightsquigarrow_c e_5^{MUX}$.

By definition, the \rightsquigarrow_c relationship does not hold between the remaining non-communication (events recorded in) log entries of c_Y and the communication log entries of c_X . However, since all log entries of c_Y are ultimately the consequence of the log entries of c_X , we can speculate that a sequence of non-communication log entries $\langle ne_1^Y, ne_2^Y, \dots, ne_k^Y \rangle$ of c_Y after a communication log entry ce^Y of c_Y is also related to the most recent communication log entry ce^X of c_X . More precisely, if we have a log $\langle \dots, ce^Y, ne_1^Y, ne_2^Y, \dots, ne_k^Y, ce^Y, \dots \rangle$ of c_Y where $ce^X \rightsquigarrow_c ce^Y$, we say that ce^X *leads-to* $\langle ce^Y, ne_1^Y, ne_2^Y, \dots, ne_k^Y \rangle$, denoted with $ce^X \rightsquigarrow \langle ce^Y, ne_1^Y, ne_2^Y, \dots, ne_k^Y \rangle$. When considering *TC* and *MUX* in the first execution of our running example, we have $e_1^{TC} \rightsquigarrow \langle e_1^{MUX}, e_2^{MUX}, e_3^{MUX}, e_4^{MUX} \rangle$ because $e_1^{TC} \rightsquigarrow_c e_1^{MUX}$ (as identified above); also, we have $e_2^{TC} \rightsquigarrow \langle e_5^{MUX} \rangle$ because $e_2^{TC} \rightsquigarrow_c e_5^{MUX}$ and there are no further non-communication log entries after e_5^{MUX} . Table I shows all the log entries dependencies extracted for the log entries in Figure 2.

We remark that our heuristic may introduce some imprecisions, for example, with logs in which the timestamp granularity is relatively coarse-grained (e.g., seconds instead of milli- or nano-seconds) and the communication between components is fast enough such that often two communication events that logically occur one before the other are logged using the same timestamp. Incorrectly identified log entries dependencies can decrease the accuracy of the resulting system-level model and increase its complexity; we leave the study of more accurate techniques for the identification of log entries dependencies as part of future work.

²We assume that the clocks of the different components are synchronized, for example using the Network Time Protocol (NTP) [17].

Algorithm 1 STITCH

Input: Set of Components $C = \{c_{main}, c_1, \dots, c_n\}$
 Set of gFSMs $M = \{m_{c_{main}}, m_{c_1}, \dots, m_{c_n}\}$
 Set of Logs $L_{main} = \{l_1, \dots, l_k\}$

Output: System model m_{sys}

- 1: Set of gFSMs $W \leftarrow \emptyset$
 - 2: **for each** $l_i \in L_{main}$ **do**
 - 3: gFSM $m_{main} \leftarrow \text{GRAFT}(c_{main}, l_i, M)$
 - 4: $W \leftarrow \{m_{main}\} \cup W$
 - 5: **end for**
 - 6: gFSM $m_{sys} \leftarrow \text{DFAUnion}(W)$
 - 7: **return** m_{sys}
-

B. Stitching Stage

The intermediate outputs of the pre-processing stage are then used in this *stitching* stage, which is at the core of our technique. In this stage, we build a system-level gFSM that captures not only the components' behavior inferred from the logs but also their dependencies as reflected in the log entries dependencies identified in the pre-processing stage.

Since the dependencies between components observed through the logs are different from execution to execution, we first build system-level gFSM *for each execution* and then merge these gFSMs together using the standard DFA (Deterministic Finite Automaton) union operation³. We call this process “stitching” whereas we call “grafting” the inner process that builds a system-level gFSM for each execution. The pseudocode of the top-level process STITCH is shown in Algorithm 1. We assume that, within a set of components C , there is a component labeled c_{main} that corresponds to the root component in the system architectural diagram (e.g., TC in our running example). Algorithm STITCH takes as input C , a set of component-level gFSMs M (one model for each component in C), and a set of logs (one log for each execution) L_{main} for c_{main} ; it returns a system-level gFSM m_{sys} . Internally, STITCH uses novel auxiliary algorithms (GRAFT, SLICE, INSERT), which are described further below.

The algorithm builds a system-level gFSM m_{main} for each execution log $l_i \in L_{main}$, starting from the component-level gFSMs in M (lines 1–4); this is done by the GRAFT algorithm, described in detail in § IV-B1. During the iteration through the execution logs in L_{main} , the resulting system-level gFSMs m_{main} are collected in the set W . Last, the gFSMs in W are merged into m_{sys} using the DFA union operation⁴ (line 6). The algorithm ends by returning the system-level gFSM m_{sys} (line 7), inferred from all executions in L_{main} .

1) *Graft*: The GRAFT algorithm builds the system-level gFSM for an execution by merging the individual component-level gFSMs, taking into account the log entries dependencies extracted from the execution, while preserving the component

³MINT produces a deterministic gFSM $m = (S, ET, G, \delta, s_0, F)$, with $\delta : S \times ET \times G \rightarrow S$; it can be easily converted into a DFA $m' = (S, \Sigma, \delta', s_0, F)$ with $\delta' : S \times \Sigma \rightarrow S$ where $\Sigma = ET \times G$.

⁴One could use the standard DFA minimization after the DFA union in line 6 to reduce the size of the system-level gFSM. However, our preliminary evaluation showed that the minimization operation can reduce the gFSM size (in terms of numbers of states and transitions) by at most 5%, and it increases the execution time of the STITCH algorithm by more than five times.

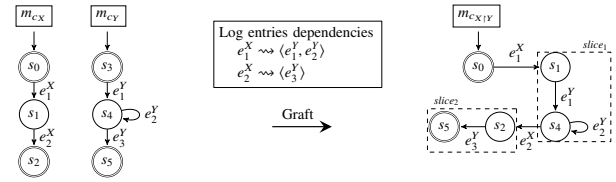


Fig. 5. The main intuition behind the GRAFT algorithm (for simplicity, we use log entries as transition labels)

Algorithm 2 Graft

Input: Component c_{cur}

Log $l_{cur} = \langle e_1, \dots, e_z \rangle$

Set of gFSMs $M = \{m_{c_{main}}, m_{c_1}, \dots, m_{c_n}\}$

Output: System model for the current execution m_{sl}

- 1: gFSM $m_{cur} \leftarrow \text{getComponentGFSM}(M, c_{cur})$
 - 2: gFSM $m_{sl} \leftarrow \text{SLICE}(m_{cur}, l_{cur})$
 - 3: State $s \leftarrow \text{getInitialState}(m_{sl})$
 - 4: **for each** $e_i \in l_{cur}$ **do**
 - 5: GuardedTransition $gt \leftarrow \text{getGuardedTran}(m_{sl}, s, e_i)$
 - 6: Set of gFSMs $W \leftarrow \emptyset$
 - 7: **for each** log entries sequence $l_d \mid e_i \rightsquigarrow l_d$ **do**
 - 8: Component $c_d \leftarrow \text{getComponentFromLog}(l_d)$
 - 9: gFSM $m_g \leftarrow \text{GRAFT}(c_d, l_d, M)$
 - 10: $W \leftarrow \{m_g\} \cup W$
 - 11: **end for**
 - 12: gFSM $m_{pl} \leftarrow \text{DFAParallelComposition}(W)$
 - 13: $m_{sl} \leftarrow \text{INSERT}(m_{sl}, gt, m_{pl})$
 - 14: $s \leftarrow \text{getTargetState}(gt)$
 - 15: **end for**
 - 16: **return** m_{sl}
-

gFSMs as much as possible. To illustrate the main idea behind the algorithm, let us consider two components c_x and c_y , whose corresponding gFSMs (inferred in the pre-processing stage) m_{c_x} and m_{c_y} are shown in Figure 5. These gFSMs respectively accept log $l_x = \langle e_1^x, e_2^x \rangle$ and log $l_y = \langle e_1^y, e_2^y, e_3^y \rangle$. Let us also assume that in terms of log entries dependencies (expressed through the *leads-to* relation) we have $e_1^x \rightsquigarrow \langle e_1^y, e_2^y \rangle$ and $e_2^x \rightsquigarrow \langle e_3^y \rangle$. Taking into account these dependencies, intuitively we can say that the gFSM resulting from the merge of m_{c_x} and m_{c_y} , denoted by $m_{c_{xy}}$, should accept the sequence of log entries $\langle e_1^x, e_1^y, e_2^y, e_2^x, e_3^y \rangle$. To obtain $m_{c_{xy}}$, we first “slice” m_{c_y} into two gFSMs: $slice_1$ (accepting $\langle e_1^y, e_2^y \rangle$) and $slice_2$ (accepting $\langle e_3^y \rangle$); then, we “insert” 1) $slice_1$ as the target of the transition of m_{c_x} that reads e_1^x , and 2) $slice_2$ as the target of the transition of m_{c_x} that reads e_2^x . Note that the self-loop transition in m_{c_y} is preserved in $m_{c_{xy}}$ as a result.

As shown in Algorithm 2, GRAFT takes as input a component c_{cur} , an execution log $l_{cur} = \langle e_1, \dots, e_z \rangle$, and a set of component-level gFSMs $M = \{m_{c_{main}}, m_{c_1}, \dots, m_{c_n}\}$; it returns a gFSM m_{sl} that accepts the sequence of log entries composed of the entries $e_i \in l_{cur}$, with each e_i interleaved with the log entries to which it *leads-to*.

The algorithm starts by slicing the gFSM $m_{c_{cur}}$ of the input component c_{cur} into a gFSM m_{sl} that accepts only l_{cur} (line 2); the actual slicing is done through algorithm SLICE, described in detail in § IV-B2. The rest of the algorithm expands m_{sl} taking into account the log entries dependencies (lines 3–14): for each log entry $e_i \in l_{cur}$, a gFSM m_g that accepts the log

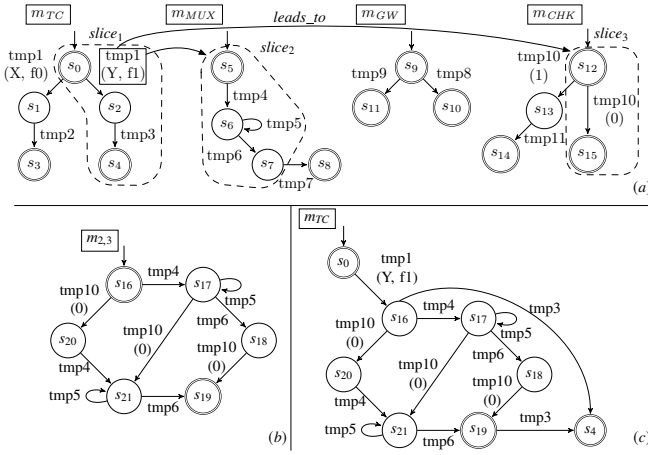


Fig. 6. Application of algorithm GRAFT to Execution-2 of the running example

entries sequence that e_i *leads-to* is built and “inserted” in m_{sl} as the target of the guarded transition gt that reads e_i . More precisely, the algorithm performs a run of m_{sl} as if it were to accept the log l_{cur} : starting from the initial state of m_{sl} (line 3), it moves to the next state s by making the guarded transition gt that reads e_i (line 5). As part of this move, for each log entry sequence l_d such that $e_i \rightsquigarrow l_d$, we recursively call GRAFT to build the gFSM m_g that accepts l_d ; this gFSM is then added to the set W (lines 7–10). Since a log entry e_i may *lead-to* log entries sequences of multiple components, we compose the individual gFSMs in W using the standard DFA parallel composition operation (line 12). The resulting gFSM m_{pl} is “inserted” in m_{sl} as the target of gt by the INSERT algorithm (line 13), described in detail in § IV-B3. At the end of each iteration of the loop, the state s is updated with the target state of the gt transition (line 14).

As an example, let us consider the case in which the STITCH algorithm calls the GRAFT algorithm when processing Execution-2 of our running example. Figure 6-(a) shows the component-level gFSM and how they are related when taking into account the *leads-to* relation listed in Table I. Algorithm STITCH invokes GRAFT with parameters $c_{cur} = TC$, $l_{cur} = \langle e_{1,2}^{TC}, e_{2,2}^{TC} \rangle$, $M = \{m_{TC}, m_{MUX}, m_{CHK}, m_{GW}\}$. The call to SLICE yields the gFSM $slice_1$ shown in Figure 6-(a); it accepts $\langle e_{1,2}^{TC}, e_{2,2}^{TC} \rangle$, using the transitions labeled with $tmp_1(Y, f1)$ and tmp_3 . Then, starting from s_0 of $slice_1$, the invocation of the auxiliary function *getGuardedTran* yields the guarded transition $(s_0, tmp_1, [Y, f1], s_2)$ that reads $e_{1,2}^{TC}$. Since $e_{1,2}^{TC} \rightsquigarrow \langle e_{1,2}^{MUX}, e_{2,2}^{MUX}, e_{3,2}^{MUX} \rangle$ and $e_{1,2}^{TC} \rightsquigarrow e_{1,2}^{CHK}$, the algorithm makes a recursive call for $\langle e_{1,2}^{MUX}, e_{2,2}^{MUX}, e_{3,2}^{MUX} \rangle$, which returns the sliced gFSM $slice_2$, and for $\langle e_{1,2}^{CHK} \rangle$, which returns $slice_3$; both gFSMs are shown in Figure 6-(a). At the end of the inner loop, we have $W = \{slice_2, slice_3\}$; their parallel composition is $m_{2,3}$ and is shown in Figure 6-(b). This gFSM is then inserted in $slice_1$ as the target of the transition $(s_0, tmp_1, [Y, f1], s_2)$, as shown in Figure 6-(c). The algorithm ends for $e_{1,2}^{TC}$ by inserting $m_{2,3}$ in s_2 and moves on to the next log entry $e_{2,2}^{TC}$.

Algorithm 3 Slice

Input: A component gFSM m_c
A component Log $l_c = \langle e_1, \dots, e_z \rangle$

Output: a sliced gFSM m_{sl}

- 1: gFSM $m_{sl} \leftarrow \text{initGFSM}()$
- 2: State $s \leftarrow \text{getSliceStartState}(m_c)$
- 3: **for each** $e_i \in l_c$ **do**
- 4: Guarded Transition $gt \leftarrow \text{getGuardedTran}(m_c, s, e_i)$
- 5: $m_{sl} \leftarrow \text{AddGuardedTranAndStates}(m_{sl}, gt)$
- 6: $s \leftarrow \text{getTargetState}(gt)$
- 7: **end for**
- 8: $\text{updateSliceStartState}(m_c, s)$
- 9: **return** m_{sl}

2) *Slice*: This algorithm takes as input a component-level gFSM m_c and a log l_c ; it returns a new gFSM m_{sl} , which is the sliced version of m_c and accepts only l_c .

Its pseudocode is shown in Algorithm 3. First, the algorithm retrieves the state of m_c that will become the initial state s of the sliced gFSM m_{sl} (line 2). Upon the first invocation of SLICE for a certain gFSM m_c , s will be the initial state of m_c ; for the subsequent invocations, s will be the last state visited in m_c when running the previous slice operations. Starting from s , the algorithm performs a run of m_c as if it were to accept the log l_c : the traversed states and guarded transitions of m_c are added into m_{sl} (lines 3–6). At the end of the loop, the algorithm records (line 8) the last state visited in m_c when doing the slicing, which will be used as the initial state of the next slice on m_c ; it then ends by returning m_{sl} .

3) *Insert*: We recall that this algorithm is invoked by the GRAFT algorithm to “insert” a gFSM m_y into a gFSM m_x as the target of a guarded transition gt of m_x , taking into account the log entries dependencies. More specifically, let us consider a log entry e and a set of logs $L = \{l_1, \dots, l_n\}$ where $e \rightsquigarrow l_i$ for $i = 1, \dots, n$; the transition gt of m_x reads e , and m_y is the parallel composition of the gFSMs that accepts the logs in L . The INSERT algorithm merges m_y into m_x such that, by “inserting” m_y as the target of the guarded transition gt , m_x can read the (entries in the) logs in L right after reading e .

We illustrate how the algorithm works through the example in Figure 7, in which the input gFSMs m_x and m_y are shown on the left side; we will insert m_y into m_x as the target of the guarded transition gt , labeled with a and having s_t as target state. Without loss of generality, we assume that m_y has only one transition (labeled with α) between its initial state s_i and the final one s_f . The main idea behind the INSERT algorithm is to duplicate both incoming and outgoing transitions of the target state of gt , and to redirect the new copies to the initial and final states of m_y . More specifically:

- the incoming transition gt of s_t (labeled with a) is duplicated and the new copy is redirected, by changing its target state, to the initial state of m_y (i.e., s_i);
- the outgoing transitions of s_t (e.g., the one labeled with b) are duplicated and the new copies are redirected, by changing the source state, such that they originate from the final state of m_y (i.e., s_f).

The updated m_x , resulting from the application of duplication and redirection, is shown in the middle of Figure 7. We

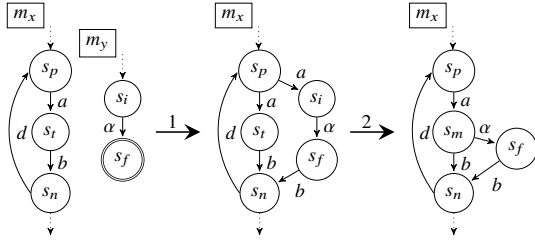


Fig. 7. Example showing the basic idea of the INSERT algorithm, when inserting m_y into m_x as the target of the guarded transition gt with $gt = (s_p, a, s_t)$. Step 1 shows the application of duplication and redirection; step 2 applies determinization to merge states s_t and s_i .

Algorithm 4 Insert

Input: gFSM m_x
Guarded Transition gt
gFSM m_y
Output: Updated gFSM m_x

- 1: State $s_t \leftarrow \text{getTargetState}(gt)$
- 2: State $s_i \leftarrow \text{getInitialState}(m_y)$
- 3: Set of States $F_y \leftarrow \text{getFinalStates}(m_y)$
- 4: **for each** Guarded Transition t of s_t **do**
- 5: **if** $t = gt$ **then**
- 6: $\text{duplicateAndRedirectTransitions}(t, s_t, \{s_i\})$
- 7: **else if** t is an outgoing transition **then**
- 8: $\text{duplicateAndRedirectTransitions}(t, s_x, F_y)$
- 9: **end if**
- 10: **end for**
- 11: $\text{determinization}(m_x)$
- 12: **return** m_x

remark that we keep the original incoming and outgoing transitions of s_t on purpose, to take into account the cases in which one of the log entries read by gt does not *lead-to* log entries read by the transition labeled with α . Duplication and redirection operations introduce some nondeterminism in m_x ; in our example, s_p has two outgoing transitions both labeled with a . We remove nondeterminism using a *determinization* procedure [18], which recursively merges pair of states that introduces nondeterminism⁵; in our example, the determinization procedure will merge s_t and s_i . The final m_x is shown on the right side of Figure 7.

Algorithm 4 shows the pseudocode of the INSERT algorithm. The algorithm takes a gFSM m_x , a guarded transition gt , and a gFSM m_y ; it returns the updated m_x that includes m_y as the target of gt . In the algorithm, s_t is the target state of gt , s_i is the initial state of m_y and F_y is the set of the final states of m_y . The core part (lines 4–10) iterates through each guarded transition t of s_t , duplicates it, and redirects the new copy as described above, using the the auxiliary function $\text{duplicateAndRedirectTransitions}$. Last, the algorithm removes nondeterminism using determinize (line 11); it ends by returning the updated gFSM m_x (line 12).

Accuracy of the system-level gFSM: *SCALER* has three main sources of over-generalization that reduce the accuracy: (1) component-level model inference, (2) parallel composition in GRAFT, and (3) determinization in INSERT. The first is

⁵This procedure is different from the standard NFA (non-deterministic finite automaton) to DFA conversion since it yields an automaton which may accept a more general language than the NFA it starts from [18].

essentially inevitable in any model inference algorithm; we try to compensate it by using a state-of-the-art tool (MINT) to infer component models that are as accurate as possible. The second source may become a problem when the log dependencies identified in the preprocessing stage are incorrect; nevertheless, over-generalization caused by parallel composition is limited because the latter is only performed on the sliced gFSMs. The last source has limited effects because recursive determinization rarely occurs in practice.

We further discuss the accuracy of *SCALER* corroborated by experimental data in the next section.

V. EVALUATION

We have implemented the *SCALER* approach as a Python program. In this section, we report on the evaluation of the performance of the *SCALER* implementation in generating the model of a component-based system from the individual component-level logs.

First, we assess the scalability of *SCALER* in inferring models from large execution logs. This is the primary dimension we focus on since we propose *SCALER* as a viable alternative to state-of-the-art techniques for processing large logs. Second, we analyze how accurate the models generated by *SCALER* are. This is an important aspect because it is orthogonal to scalability and has direct implications on the possibility of using the models generated by *SCALER* in other software engineering tasks (e.g., test case generation). Summing up, we investigate the following research questions:

- RQ1: *How scalable is SCALER when compared to state-of-the-art model inference techniques?*
RQ2: *How accurate are the models (in the form of gFSMs) generated by SCALER when compared to those generated by state-of-the-art model inference techniques?*

A. Benchmark and Evaluation Settings

We used a benchmark composed of industrial, proprietary datasets provided by one of our industrial partners, active in the satellite industry. The benchmark contains component-level logs recorded during the execution of a satellite ground control system, which includes six major components. We created the benchmark as follows. First, we executed system-level tests on the ground control system 120 times and, in each test execution, we collected the log files of the six major components. Then, we created seven datasets of size ranging from 5K to 35K, where the size is expressed in terms of the total number of log entries. We assembled each dataset by randomly selecting a number of executions out of the pool of 120 executions, such that the total size of the logs contained in the dataset matched the desired dataset size. By construction, each dataset contains logs of the six major components of the system. The first three columns of Table II show, for each dataset in our benchmark, the size and the number of executions included in it. In total, there are 92 unique templates (i.e., unique number of events) for all logs. All the collected logs (anonymized) as well as the evaluation results are available at <http://tiny.cc/SANER20-SCALER>. The experiments have been

executed on a high-performance computing platform, using one of its quad-core nodes running CentOS 7 on a 2.40 GHz Intel Xeon E5-2680 v4 processor with 4 GB memory.

B. Scalability

1) *Methodology*: To answer RQ1, we assess the scalability of *SCALER*, in terms of execution time with respect to the size of the logs, in comparison with MINT [8], a state-of-the-art model inference tool. We selected MINT as baseline because other tools are either not publicly available or require information not available in most practical contexts, including ours (e.g., channels’ definitions; see section III).

We ran both tools to infer a system-level model for each dataset in our benchmark. We provided as input to *SCALER* 1) the logs of the six components recorded in the executions contained in each dataset; 2) the architectural dependencies among components; 3) the list of log message templates for communication events, received from a domain expert. As for MINT, we provided as input the system-level logs of the system executions contained in each dataset. We derived these system-level logs by linearizing the individual component logs in each execution, taking into account the log entries dependencies. To guarantee a fair comparison, these dependencies are the same as those extracted in the pre-processing stage of *SCALER*. Since the total number of possible system-level logs is extremely large due to the linearization of the parallel behaviors of the components, we only considered one system-level log for each execution.

We remark that we used *two* instances of MINT: the one used internally by *SCALER* to generate component-level models; the other one for the comparison in inferring system-level models. For both instances, we used the default configuration (i.e., state merging threshold $k = 2$ and J48 as data classifier algorithm) [8]. Furthermore, to identify the event templates required by the MINT instances to parse the log entries, we first used a state-of-the-art tool (MoLFI [13]) to compute them and then we asked a domain expert to further refine them, e.g., by collapsing similar templates into a single one. To take into account the randomness of the log linearization (i.e., only one linearized system-level log) for each execution of MINT, we ran both MINT and *SCALER* ten times on each dataset. For each run, we set an overall time out of 24h for the model inference process both for MINT and for *SCALER*.

To assess the statistical significance of the difference between the execution time of *SCALER* and MINT (if any), we used the non-parametric Wilcoxon rank sum test with a level of significance $\alpha = 0.05$. Furthermore, we used the Vargha-Delaney (\hat{A}_{12}) statistic for determining the effect size of the difference. In our case, $\hat{A}_{12} < 0.5$ indicates that the execution time of *SCALER* is lower than that of MINT.

2) *Results*: The columns under the header “Scalability” of Table II show the scalability results for *SCALER* and MINT. More precisely, column *MINT* indicates the execution time of MINT; columns *Prep*, *Stitch*, and *Total* indicate the average (over the ten runs) execution time (in seconds) and the corresponding standard deviation of *SCALER* for the pre-processing

stage, the stitching stage, and the cumulative execution time, respectively; column *SpeedUp* reports the speedup of *SCALER* over MINT computed as $\frac{Time_{MINT}}{Time_{SCALER}}$ [19].

SCALER is faster than MINT for all the datasets in our benchmark; the speed-up ranges between 27x (for the dataset D05K) and 428x (for the dataset D25K). The speed-up increases with the size of the datasets and, thus, the benefit of using *SCALER* over MINT increases for larger logs. Note that MINT reached the time out for the largest dataset (D35K) without producing any model. The Wilcoxon test also confirms that the differences in execution time between *SCALER* and MINT are statistically significant (p -value < 0.01 for all datasets) and the Vargha-Delaney statistic indicates that the effect size is always *large* ($\hat{A}_{12} < 0.10$) for all datasets.

Analyzing the performance of the two instances of MINT, we can say that when MINT is used for component-level model inference is much faster than MINT used for system-level model inference because (1) the component logs are smaller than the system-level logs and (2) there is a higher similarity among component logs than system-level logs.

C. Accuracy

1) *Methodology*: To answer RQ2, we ran both MINT and *SCALER* to evaluate and compare their accuracy for each dataset, in terms of recall and specificity of the inferred models following previous studies [8]–[10]. Recall measures the ability of the inferred models of a system to accept “positive” logs; specificity measures the ability of the inferred models to reject “negative” logs. We computed these metrics by using the well-known k -folds cross validation method, which has also been used in previous work [8]–[10] in the area of model inference. This method randomly partitions a set of logs into k non-overlapping folds; $k - 1$ folds are used as input of the model inference tool, while the remaining fold is used as “test set”, to check whether the model inferred by the tool accepts the logs in the fold. The procedure is repeated k times until all folds have been considered exactly once as the test set. For each fold, if the inferred model successfully accepts a positive log in the test set, the positive log is classified as True Positive (TP); otherwise, the positive log is classified as False Negative (FN). Similarly, if an inferred model successfully rejects a negative log in the test set, the negative log is classified as True Negative (TN); otherwise, the negative log is classified as False Positive (FP). Based on the classification results, we calculated the recall (R) as $R = \frac{|TP|}{|TP|+|FN|}$, and the specificity (S) as $S = \frac{|TN|}{|TN|+|FP|}$.

As done in previous work [8]–[10], we synthesized negative logs from positive logs by introducing small changes (mutations): 1) swapping two randomly selected log entries, 2) deleting a randomly selected log entry, and 3) adding a log entry randomly selected from other executions. To make sure a log resulting from a mutation contains invalid behaviors of the system, we checked whether the sequence of entries around the mutation location (i.e., the mutated entries and the entries immediately before and after the mutants) did not also appear in the positive logs.

TABLE II
EXECUTION TIME (IN SECONDS), RECALL, AND SPECIFICITY OF *SCALER* AND MINT

Dataset	Size Exec		System-level gFSM							Scalability				Accuracy						
			States			Transitions				MINT	<i>SCALER</i>			SpeedUp	Recall			Specificity		
			MINT	<i>SCALER</i>	Ratio	MINT	<i>SCALER</i>	Ratio	Prep(s)		Stitch(s)	Total(s)	MINT		<i>SCALER</i>	$\Delta_R(pp)$	MINT	<i>SCALER</i>	$\Delta_S(pp)$	
D05K	5058	13	617.7	3816	6.2	837.2	7295	8.7	319.6	6.0	5.8	11.8	27.1	0.09	0.65	56	1.00	0.98	-2	
D10K	10208	28	1207.3	6647	5.5	1585.4	12720	8.0	2597.0	10.9	15.3	26.2	99.2	0.16	0.63	47	0.99	0.98	-1	
D15K	15078	42	1582.6	4184	2.6	2064.4	8868	4.3	7403.8	13.4	19.8	33.2	222.8	0.52	0.82	30	0.99	0.97	-2	
D20K	20094	56	2257.0	7463	3.3	2914.7	15851	5.4	16022.2	18.6	32.1	50.7	315.9	0.58	0.86	28	0.98	0.97	-1	
D25K	25034	71	3067.2	9496	3.1	3976.3	18767	4.7	35378.6	24.3	58.2	82.5	428.7	0.56	0.83	27	0.98	0.96	-2	
D30K	30103	86	2871.3	19467	6.8	3701.8	40204	10.9	59222.7	29.0	129.6	158.6	373.3	0.61	0.86	25	0.98	0.96	-2	
D35K	35079	101	N/A	10432	N/A	N/A	19707	N/A	timeout	32.5	72	104.5	N/A	N/A	0.88	N/A	N/A	0.97	N/A	
Avg	20093.4	56.7	1933.9	8786.4	4.6	2513.3	17630.3	7.0	20157.3	19.3	47.5	66.8	244.5	0.42	0.79	35.5	0.99	0.97	-1.67	

Note that we needed to derive system-level logs from the individual component logs in test sets to check the acceptance of the system-level models inferred by *SCALER* and MINT. To this end, as done for the scalability evaluation, for each execution in the test sets, we linearized the individual component logs to derive the system-level log. Also, to take into account the randomness of the derivation of system-level logs, we repeat the 10-folds cross validation ten times on each dataset and then applied statistical tests as done for the scalability evaluation.

2) *Results*: The columns under the header “Accuracy” of Table II show the results of MINT and *SCALER* in terms of recall, specificity, and difference of these values (in percentage points, *pp*) between *SCALER* and MINT.

MINT achieves high specificity scores, always greater than 0.98. However, recall is low, ranging between 0.09 for the D05K dataset and 0.61 for the D30K dataset. Notice that no results were obtained for the larger dataset with 35K log entries because MINT reached the timeout of 24h without generating any model. *SCALER* achieves a slightly lower specificity than MINT, with an average difference of 1.67*pp*. However, *SCALER* achieves substantially higher recall than MINT. The difference in recall values ranges between +25*pp* (D30K dataset) and +56*pp* (D05K dataset), with an average improvement of 35.5*pp*. Such a result can be explained mainly because MINT takes as input only one system-level log among all possible instances of the linearization of the parallel behaviors of the components for each execution, and fails to scale up to take as input all the possible system-level logs. Related to this, since *SCALER* takes as input all the possible system-level logs (in the form of component-level logs with the log entries dependencies) for each execution, it returns as output a system-level gFSM having on average 4.6x more states and 7.0x more transitions than MINT (see the columns under the header “System-level gFSM” in Table II).

According to the Wilcoxon test, *SCALER* always achieves a statistically higher recall than MINT for all datasets (*p*-value < 0.01) with a large effect size. However, *SCALER* achieves a statistically lower specificity than MINT in five out of seven

datasets (i.e., with 5K, 10K, 20K and 30K log entries). While the difference in specificity are statistically significant, it is worth noting that the magnitude of the difference is small, being no larger than 2*pp*.

D. Discussion and Threats to Validity

From the results above, we conclude that, for the large logs typically encountered in practice, *SCALER* provides results that are good enough to generate nearly correct (with a specificity always greater than 0.96) and largely complete models (with an average recall of 0.79).

The incompleteness of the inferred models is due to the limited knowledge we have on the system (i.e., the incomplete list of message templates characterizing communication events) and to the heuristic used in computing log entries dependencies, which is affected by the coarse-grained timestamp granularity of the logs included in our benchmark. In contrast, MINT, when used as a stand-alone tool on the same large logs, does not scale and fares poorly in terms of recall, generating very incomplete models.

From a practical perspective, the results achieved by *SCALER* lead to a considerable reduction of false negatives, with a marginal increment of false positives. For example, for the D15K dataset, MINT generates (in about two hours) a gFSM that accepts only 52% of the true positives (positive logs). In this case, engineers need to substantially modify the inferred gFSM to accept the remaining 48% of positive logs. Instead, for the same dataset, *SCALER* generates in about 33 seconds a gFSM that accepts 82% of the positive logs (and rejects 97% of the negative logs). The marginal decrement of the negative logs correctly dismissed by the gFSM inferred by *SCALER* is largely compensated by (1) a significant reduction of the number of wrongly rejected positive logs (+30*pp* in recall), and (2) a substantial reduction of the execution time (*SCALER* is about 222 times faster than MINT).

In terms of threats to validity, the size of the log files is a confounding factor that could affect our results (i.e., accuracy and execution time). We mitigated such a threat by considering

seven datasets with different sizes (ranging from 5K to 35K log entries) and different sets of system executions.

VI. RELATED WORK

Starting from the seminal work of Biermann and Feldman [5] on the *k-Tail* algorithm, which is based on the concept of state merging, several approaches have been proposed to infer a Finite State Machine (FSM) from execution traces or logs. *Synoptic* [6] uses temporal invariants, mined from execution traces, to steer the FSM inference process to find models that satisfy such invariants; the space of the possible models is then explored using a combination of model refinement and coarsening. *InvariMINT* [20] is an approach enabling the declarative specification of model inference algorithms in terms of the types of properties that will be enforced in the inferred model; the empirical results show that the declarative approach outperforms procedural implementations of *k-Tail* and *Synoptic*. Nevertheless, this approach requires prior knowledge of the properties that should hold on the inferred model; such a pre-condition cannot be satisfied in contexts (like the one in which this work is set) where system components are black-boxes and the knowledge about the system is limited. Other approaches infer other types of behavioral models that are richer than an FSM. *GK-tail+* [9] infers guarded FSM (gFSM) by extending the *k-Tail* algorithm and combining it with Daikon [21] to synthesize constraints on parameter values; such constraints are represented as guards of the transitions of the inferred model. *MINT* [8] also infers a gFSM by combining EDSM (Evidence-Driven State Merging) [22] and data classifier inference [23]. EDSM, based on the Blue-Fringe algorithm [14], is a popular and accurate model inference technique, which won the Abbadingo [14] and the StaMinA competition [24]. Data-classifier inference identifies patterns or rules between data values of an event and its subsequent events. Using data classifiers, the data rules and their subsequent events are explicitly tied together. *ReHMM* (Reinforcement learning-based Hidden Markov Modeling) [10] infers a gFSM extended with transition probabilities, by using a hybrid technique that combines stochastic modeling and reinforcement learning. ReHMM is built on top of MINT; differently from the latter, it uses a specific data classifier (Hidden Markov model) to deal with transition probabilities. All the aforementioned approaches cannot avoid scalability issues due to the intrinsic computational complexity of inferring FSM-like models; the minimal consistent FSM inference is NP complete [25] and all of the practical approaches are approximation algorithm with polynomial complexity.

Model inference has also been proposed in the context of distributed and concurrent systems. *CSight* [12] infers a communicating FSM from logs of vector-timestamped concurrent executions, by mining temporal properties and refining the inferred model in a way similar to *Synoptic*. *MSGMiner* [26] is a framework for mining graph-based models (called Message Sequence Graphs) of distributed systems; the nodes of this graph correspond to Message Sequence Chart, whereas the edges are determined using automata learning techniques. This

work has been further extended [27] to infer (symbolic) class level specifications. However, these approaches require the availability of channel definitions, i.e., which events are used to send and receive messages among components.

Liu and Dongen [28] uses a *divide and conquer* strategy, similar to the one in our *SCALER* approach, to infer a system-level, hierarchical process model (in the form of a Petri net with nested transitions) from the logs of interleaved components, by leveraging the calling relation between the methods of different components. This approach assumes the knowledge of the caller and callee of each component methods; in our case, we do not have this information and rely on the *leads-to* relation among log entries, computed from high-level architectural descriptions and information about the communication events.

One way to tackle the intrinsic scalability issue of (automata-based) model inference is to rely on distributed computing models, such as MapReduce [29], by transforming the sequential model inference algorithms into their corresponding distributed version. In the case of the *k-Tail* algorithm, the main idea [11] is to parallelize the algorithm by dividing the traces into several groups, and then run an instance of the sequential algorithm on each of them. A more fine-grained version [7] parallelizes both the trace slicing and the model synthesis steps. Being based on MapReduce, both approaches require to encode the data to be exchanged between mappers and reducers in the form of key-value pairs. This encoding, especially in the trace slicing step, is application-specific; hence, it cannot be used in contexts in which the system is treated as a black-box, with limited information about the data recorded in the log entries. Furthermore, though the approach can infer a FSM from large logs of over 100 million events, the distributed model synthesis can be significantly slower for $k \geq 2$, since the underlying algorithm is exponential in k .

VII. CONCLUSION

In this paper, we addressed the scalability problem of inferring the model of a component-based system from the individual component-level logs, assuming only limited (and possibly incomplete) knowledge about the system. Our approach, called *SCALER*, first infers a model of each system component from the corresponding logs; then, it merges the individual component models together taking into account the dependencies among components, as reflected in the logs. Our evaluation, performed on logs from an industrial system, has shown that *SCALER* can process larger logs, is faster, and yields more accurate models than a state-of-the-art technique.

As part of future work, we plan to refine the heuristics used for identifying the dependencies of the log entries between multiple components, to take into account logs with imprecise timestamps and out-of-order messages. We also plan to evaluate *SCALER* on different datasets and to integrate it with other model inference techniques. Finally, we will assess the effectiveness of the inferred models in software engineering activities, such as test case generation.

ACKNOWLEDGMENT

This work has received funding from the European Research Council under the European Union’s Horizon 2020 research and innovation programme (grant agreement No 694277), from the Luxembourg National Research Fund (FNR) under grant agreement No C-PPP17/IS/11602677, and from a research grant by SES.

REFERENCES

- [1] J. E. Cook and A. L. Wolf, “Discovering models of software processes from event-based data,” *ACM Trans. Softw. Eng. Methodol.*, vol. 7, no. 3, pp. 215–249, 1998.
- [2] G. Fraser and N. Walkinshaw, “Behaviourally adequate software testing,” in *Proceedings of the 5th International Conference on Software Testing, Verification and Validation (ICST 2012)*. Piscataway, NJ, USA: IEEE, 2012, pp. 300–309.
- [3] E. M. Clarke Jr, O. Grumberg, D. Kroening, D. Peled, and H. Veith, *Model checking*. MIT press, 2018.
- [4] N. Walkinshaw, K. Bogdanov, C. Damas, B. Lambeau, and P. Dupont, “A framework for the competitive evaluation of model inference techniques,” in *Proceedings of the First International Workshop on Model Inference In Testing (MIIT 2010)*. New York, NY, USA: ACM, 2010, pp. 1–9.
- [5] A. W. Biermann and J. A. Feldman, “On the synthesis of finite-state machines from samples of their behavior,” *IEEE Trans. Comput.*, vol. 100, no. 6, pp. 592–597, 1972.
- [6] I. Beschastnikh, Y. Brun, S. Schneider, M. Sloan, and M. D. Ernst, “Leveraging existing instrumentation to automatically infer invariant-constrained models,” in *Proceedings of the 19th ACM SIGSOFT Symposium and the 13th European Conference on Foundations of Software Engineering (ESEC/FSE 2011)*. New York, NY, USA: ACM, 2011, pp. 267–277.
- [7] C. Luo, F. He, and C. Ghezzi, “Inferring software behavioral models with mapreduce,” *Sci. Comput. Program.*, vol. 145, pp. 13–36, 2017.
- [8] N. Walkinshaw, R. Taylor, and J. Derrick, “Inferring extended finite state machine models from software executions,” *Empir. Softw. Eng.*, vol. 21, no. 3, pp. 811–853, 2016.
- [9] L. Mariani, M. Pezzè, and M. Santoro, “Gk-tail+ an efficient approach to learn software models,” *IEEE Trans. Softw. Eng.*, vol. 43, no. 8, pp. 715–738, 2017.
- [10] S. S. Emam and J. Miller, “Inferring extended probabilistic finite-state automaton models from software executions,” *ACM Trans. Softw. Eng. Methodol.*, vol. 27, no. 1, pp. 4:1–4:39, 2018.
- [11] S. Wang, D. Lo, L. Jiang, S. Maoz, and A. Budi, “Scalable parallelization of specification mining using distributed computing,” in *The Art and Science of Analyzing Software Data*. Morgan Kaufmann, 2015, pp. 623–648.
- [12] I. Beschastnikh, Y. Brun, M. D. Ernst, and A. Krishnamurthy, “Inferring models of concurrent systems from logs of their behavior with CSight,” in *Proceedings of the 36th International Conference on Software Engineering (ICSE 2014)*. New York, NY, USA: ACM, 2014, pp. 468–479.
- [13] S. Messaoudi, A. Panichella, D. Bianculli, L. Briand, and R. Sasnauskas, “A search-based approach for accurate identification of log message formats,” in *Proceedings of the 26th International Conference on Program Comprehension (ICPC 2018)*. New York, NY, USA: ACM, 2018, pp. 167–177.
- [14] K. J. Lang, B. A. Pearlmutter, and R. A. Price, “Results of the Abbadingo One DFA learning competition and a new evidence-driven state merging algorithm,” in *Proceedings of the 4th International Colloquium on Grammatical Inference (ICGI 1998)*, ser. LNCS, vol. 1433. Berlin, Heidelberg: Springer, 1998, pp. 1–12.
- [15] J. Whaley, M. C. Martin, and M. S. Lam, “Automatic extraction of object-oriented component interfaces,” in *Proceedings of the ACM SIGSOFT International Symposium on Software Testing and Analysis (ISSTA 2002)*. New York, NY, USA: ACM, 2002, pp. 218–228.
- [16] L. C. Briand, Y. Labiche, and J. Leduc, “Toward the reverse engineering of UML sequence diagrams for distributed Java software,” *IEEE Trans. Softw. Eng.*, vol. 32, no. 9, pp. 642–663, 2006.
- [17] D. L. Mills, “Internet time synchronization: The network time protocol,” *Transactions on Communications*, vol. 39, no. 10, pp. 1482–1493, 1991.
- [18] C. Damas, B. Lambeau, P. Dupont, and A. van Lamsweerde, “Generating annotated behavior models from end-user scenarios,” *IEEE Trans. Softw. Eng.*, vol. 31, no. 12, pp. 1056–1073, 2005.
- [19] S. Sahni and V. Thanvantri, “Performance metrics: Keeping the focus on runtime,” *IEEE Parallel Distributed Technology: Systems Applications*, vol. 4, no. 1, pp. 43–56, 1996.
- [20] I. Beschastnikh, Y. Brun, J. Abrahamson, M. D. Ernst, and A. Krishnamurthy, “Using declarative specification to improve the understanding, extensibility, and comparison of model-inference algorithms,” *IEEE Trans. Softw. Eng.*, vol. 41, no. 4, pp. 408–428, 2015.
- [21] M. D. Ernst, J. H. Perkins, P. J. Guo, S. McCamant, C. Pacheco, M. S. Tschantz, and C. Xiao, “The daikon system for dynamic detection of likely invariants,” *Sci. Comput. Program.*, vol. 69, no. 1, pp. 35–45, 2007.
- [22] K. Cheng and A. S. Krishnakumar, “Automatic functional test generation using the extended finite state machine model,” in *Proceedings of the 30th Design Automation Conference (DAC 1993)*. New York, NY, USA: ACM, 1993, pp. 86–91.
- [23] T. M. Mitchell, *Machine Learning*. New York, NY, USA: McGraw-Hill, Inc., 1997.
- [24] N. Walkinshaw, B. Lambeau, C. Damas, K. Bogdanov, and P. Dupont, “Stamina: A competition to encourage the development and assessment of software model inference techniques,” *Empir. Softw. Eng.*, vol. 18, no. 4, pp. 791–824, Aug 2013.
- [25] E. M. Gold, “Language identification in the limit,” *Information and Control*, vol. 10, no. 5, pp. 447–474, 1967.
- [26] S. Kumar, S. Khoo, A. Roychoudhury, and D. Lo, “Mining message sequence graphs,” in *Proceedings of the 33rd International Conference on Software Engineering (ICSE 2011)*. New York, NY, USA: ACM, 2011, pp. 91–100.
- [27] S. Kumar, S.-C. Khoo, A. Roychoudhury, and D. Lo, “Inferring class level specifications for distributed systems,” in *Proceedings of the 34th International Conference on Software Engineering (ICSE 2012)*. Piscataway, NJ, USA: IEEE, 2012, pp. 914–924.
- [28] C. Liu, B. van Dongen, N. Assy, and W. M. P. van der Aalst, “Component behavior discovery from software execution data,” in *Proceedings of the Symposium Series on Computational Intelligence (SSCI 2016)*. Piscataway, NJ, USA: IEEE, 2016, pp. 1–8.
- [29] J. Dean and S. Ghemawat, “Mapreduce: Simplified data processing on large clusters,” *Commun. ACM*, vol. 51, no. 1, pp. 107–113, 2008.